Observation of Magnetic Octupole Decay in Atomic Spectra

P. Beiersdorfer, A. L. Osterheld, J. Scofield, B. Wargelin, and R. E. Marrs
University of California, Lawrence Livermore National Laboratory, Livermore, California 94550
(Received 9 July 1991)

We report the first observation of magnetic octupole decay in the x-ray spectrum of a highly charged ion. Detailed analyses of the low-energy region of the $n=3\rightarrow 4$ spectra of nickel-like Th^{62+} and U^{64+} show an intense line at 2558.7 ± 0.2 and 2689.3 ± 0.2 eV, respectively, that is attributed to the transition $(3d^9 4s)_{J=3}\rightarrow(3d^{10})_{J=0}$. Calculations indicate that the line is almost exclusively excited by indirect processes such as radiative cascades and electron capture.

PACS numbers: 32.70.−n, 31.20.−d, 32.30.Rj

Transitions that do not proceed via electric dipole ($E1$) decay are of special interest in various branches of physics. Observations of these so-called "forbidden" transitions provide fundamental tests of atomic structure theory as well as checks of level population calculations. Because the intensity of forbidden transitions is sensitive to the electron density, the lines are used as a diagnostic tool in the spectroscopy of solar, astrophysical, and laser-produced plasmas.

Forbidden transitions having magnetic dipole ($M1$), magnetic quadrupole ($M2$), or electric quadrupole ($E2$) multipolarity have been observed in the x-ray spectra of highly charged ions produced in high-temperature, low-density plasma sources such as tokamaks [1] and the Sun [2]. Moreover, electric quadrupole transitions have been observed in high-density laser-produced plasmas [3] and in beam-foil interactions [4]. The latter technique has also enabled the observation of the two-photon decay of atomic levels in highly charged ions [5].

In this Letter we report the observation of magnetic octupole ($M3$) decay in an atomic system. The ions studied are nickel-like Th^{62+} and U^{64+}. Nickel-like ions have 28 remaining electrons, which, in the ground state, are arranged in the closed-shell configuration $1s^2 2s^2 2p^6 3s^2 3p^6 3d^{10}$. The lowest excited levels have an optical electron in the $4s$ subshell and a $3d_{3/2}^4 3d_{5/2}^5$ core. Levels with a $4p$ optical electron or those with a $3d_{3/2}^{-1}$ core have higher energies. A diagram of the lowest eight excited levels in U^{64+} is shown in Fig. 1. Selection rules for $E1$ decay require a change in total angular momentum $\Delta J=\pm1$, as well as a change in parity. As a result, dipole decay to the ground state of the lowest seven levels is forbidden. The $3d^{-1}4p$ levels at 2836 and 2837 eV, for example, decay instead via allowed $\Delta n=0$ $E1$ transitions to the $3d^{-1}4s$ levels. This option is unavailable to the lowest two excited levels $(3d_{5/2}^{-1}4s)_{J=2}$ and $(3d_{5/2}^{-1}4s)_{J=3}$. In the absence of collisions, these levels must decay to the ground state and must do so via an $E2$ and $M3$ transition, respectively.

The radiative rates for the $E2$ and $M3$ transitions have been calculated with the multiconfiguration relativistic atomic structure code GRASP [6] and equal 3.3×10^{10} and 1.3×10^5 s^{-1}. To predict the relative intensities of the nickel-like $4\rightarrow3$ transitions and to determine the effect of electron collisions, a complex collisional-radiative model was constructed from data generated with the Hebrew University–Lawrence Livermore atomic structure codes (HULLAC) [7]. The model includes all singly excited levels with a $3s^{-1}$, $3p^{-1}$, or $3d^{-1}$ core and an optical electron in the $n=4$ or 5 shell. Level populations are calculated from a balance of all radiative transitions and electron-impact excitations connecting these levels, of which there are more than 40000. The model predicts that electron collisions do not affect the population of these excited levels for electron densities below about 10^{14} cm^{-3}, as shown in Fig. 2 for monoenergetic electrons of 8 keV. Moreover, the low-lying excited levels are not populated by direct electron-impact excitation from the ground state. Instead, they are populated almost exclusively by radiative cascades from higher levels, as indicated in Fig. 1. Direct electron collisions contribute to the excitation of the $(3d_{5/2}^{-1}4s)_{J=3}$ level, for example, less than 1%. By contrast, radiative cascade feeding from high-lying levels, involving many intermediate levels, is highly effective in populating the $J=3$ level, making the $M3$ line the sixth most intense line in the nickel-like M-shell spectrum.

The experiment was carried out on the electron-beam

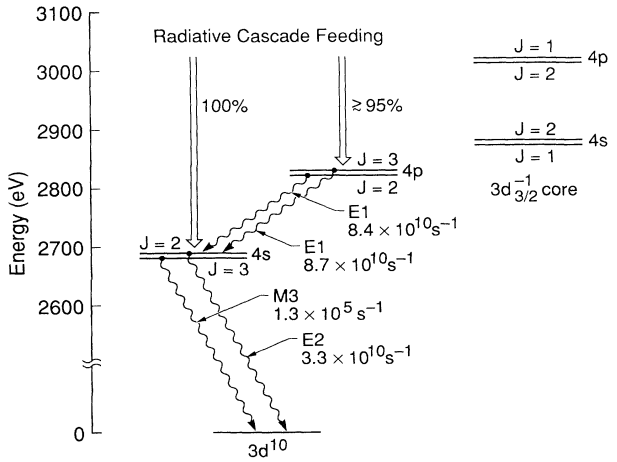

FIG. 1. Level diagram of nickel-like U^{64+} showing the lowest eight excited levels. Radiative decay rates are indicated for the four lowest levels, which have a $3d_{5/2}^{-1}$ core. These levels are populated almost exclusively by radiative cascades from higher levels.

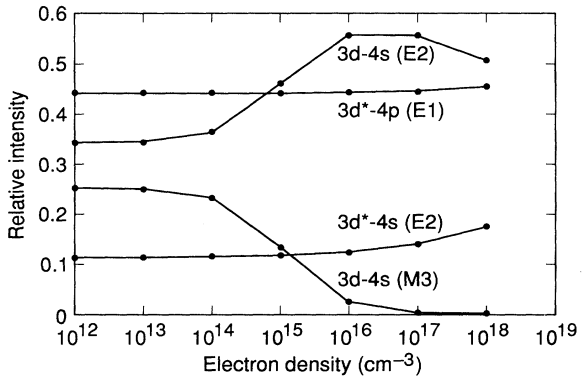

FIG. 2. Density dependence of the relative intensities of 3-4 transitions in nickel-like U^{64+}. Collisions redistribute the populations of the $3d_{5/2}^{-1}$ core levels for densities above 10^{14} cm^{-3}, diminishing the intensity of the $M3$ line in favor of the neighboring $E2$ line. Also shown are the relative intensities of the $E2$ and $E1$ transitions from excited levels five and eight (cf. Fig. 1) to the ground state involving the $3d_{5/2}^{-1}$ core, denoted $3d^*$.

ion trap (EBIT) at LLNL [8]. The device uses a 150-mA monoenergetic electron beam to generate, trap, and excite ions of the desired charge state. The beam is compressed to a 60-μm diameter so that the electron density is about 5×10^{12} cm^{-3}, i.e., low enough to observe all nickel-like transitions in the collisionless limit. X rays were analyzed with a helium-filled flat-crystal spectrometer with a Ge(111) crystal whose plane of dispersion is perpendicular to the beam direction. Observations were made in first order by setting the central Bragg angle to 47.1° for Th^{62+} and to 45.6° for U^{64+}.

The ionization potential of copperlike U^{63+} is 4.6 keV; that of nickel-like U^{64+} is 7.4 keV. Nickel-like ions, therefore, can be produced and observed for a wide range of beam energies. A survey spectrum recorded at a beam energy of 9.2 keV is shown in Fig. 3(a). It contains lines from copperlike, nickel-like, and cobaltlike transitions. A comparison with a synthetic spectrum [Fig. 3(b)] from our model calculations, which were expanded to include copperlike and cobaltlike transitions, provided positive identification of the different transitions. Our line identifications were affirmed by recording spectra for a wide range of different beam energies, for which the charge-state composition of the trapped ions varied considerably (cf. Ref. [9]).

In the survey spectrum in Fig. 3(a) the $M3$ transition in U^{64+} blends with the $E2$ transition from the next higher excited level. The line pair can be resolved with higher resolution achieved by increasing the separation between crystal and detector. A high-resolution spectrum, which clearly resolves the $M3$ transition from the neighboring $E2$ transition, is shown in Fig. 4. The transition on the low-energy side of the nickel-like transitions is due to the radiative decay of the $3d_{5/2}^{-1}4s^2$ level in copperlike U^{63+}. Unlike high-lying doubly excited levels in

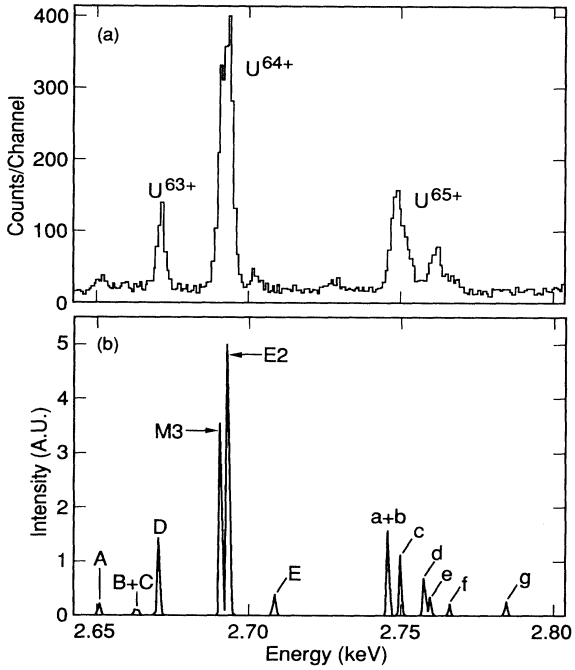

FIG. 3. (a) Survey spectrum of the 3-4 x-ray transitions in the low-energy region from near-nickel-like uranium ions obtained at an electron-beam energy of 9.2 keV. (b) Model spectrum which includes transitions from copperlike U^{63+} (uppercase letters), nickel-like U^{64+} (lines $M3$ and $E2$), and cobaltlike U^{65+} (lowercase letters). The assumed charge balance is $U^{63+}:U^{64+}:U^{65+}=1:1:1$. A listing of the transitions is given in Table I.

copperlike ions, the low-lying levels are energetically forbidden to decay via autoionization. In the absence of collisions they must decay radiatively, even via $E2$ transitions like the transition shown. A list of transitions ob-

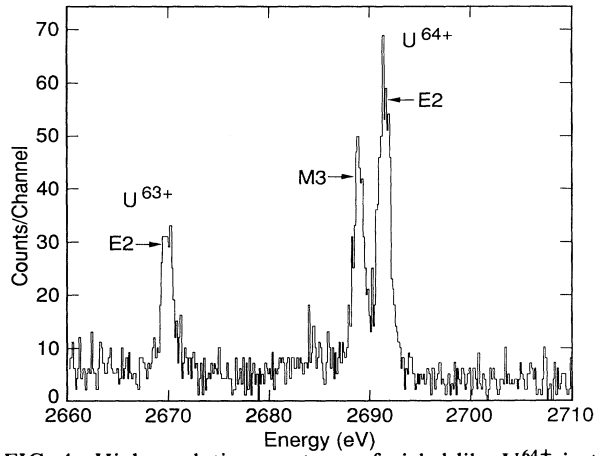

FIG. 4. High-resolution spectrum of nickel-like U^{64+} in the region 2660–2710 eV recorded at an electron-beam energy of 7.2 keV. The $E2$ and $M3$ transitions are clearly resolved. Also seen is an electric quadrupole transition in copperlike U^{63+}, labeled D in Table I.

TABLE I. Comparison of measured and calculated transition energies in copper-, nickel-, and cobaltlike thorium and uranium. All values are in eV. ⟨ · · · ⟩ denotes blend.

Key	Transition	Type	$E_{expt.}$	$E_{theor.}$	$E_{expt.}$	$E_{theor.}$
			Th^{61+}		U^{63+}	
A	$(3d_{5/2}^{-1}4s4p_{1/2})_{J=5/2} \rightarrow (4p_{1/2})_{J=1/2}$	*E*2		2520.4		2650.8
B	$(3d_{5/2}^{-1}4s4p_{1/2})_{J=5/2} \rightarrow (4p_{1/2})_{J=1/2}$	*E*2		2531.6		2662.6
C	$(3d_{5/2}^{-1}4s4p_{1/2})_{J=3/2} \rightarrow (4p_{1/2})_{J=1/2}$	*M*1		2532.4		2663.3
D	$(3d_{5/2}^{-1}4s^2)_{J=5/2} \rightarrow (4s)_{J=1/2}$	*E*2	2539.9 ± 0.2	2538.4	2670.2 ± 0.2	2669.5
E	$(3d_{3/2}^{-1}4s^2)_{J=3/2} \rightarrow (4p_{1/2})_{J=1/2}$	*E*1	2569.5 ± 0.3	2566.5	2712.8 ± 0.6	2710.3
			Th^{62+}		U^{64+}	
*M*3	$(3d_{5/2}^{-1}4s)_{J=3} \rightarrow {}^1S_{J=0}$	*M*3	2558.7 ± 0.2	2557.4	2689.3 ± 0.2	2688.4
*E*2	$(3d_{5/2}^{-1}4s)_{J=2} \rightarrow {}^1S_{J=0}$	*E*2	2561.3 ± 0.2	2560.0	2691.9 ± 0.2	2690.9
			Th^{63+}		U^{65+}	
a	$(3d_{5/2}^{-2}4s)_{J=9/2} \rightarrow (3d_{5/2}^{-1})_{J=5/2}$	*E*2	⟨2614.4 ± 0.3⟩	2613.2	⟨2745.4 ± 0.5⟩	2746.0
b	$(3d_{3/2}^{-1}3d_{5/2}^{-1}4s)_{J=5/2} \rightarrow (3d_{3/2}^{-1})_{J=3/2}$	*E*1	⟨2614.4 ± 0.3⟩	2613.8	⟨2745.4 ± 0.5⟩	2746.7
c	$(3d_{5/2}^{-2}4s)_{J=7/2} \rightarrow (3d_{5/2}^{-1})_{J=5/2}$	*E*1	2618.2 ± 0.3	2617.3	2750.9 ± 0.7	2750.3
d	$(3d_{5/2}^{-2}4s)_{J=5/2} \rightarrow (3d_{5/2}^{-1})_{J=5/2}$	*E*1	2626.7 ± 0.3	2626.3		2759.5
e	$(3d_{5/2}^{-2}4s)_{J=3/2} \rightarrow (3d_{5/2}^{-1})_{J=5/2}$	*E*1	2628.6 ± 0.3	2628.3		2761.7
f	$(3d_{3/2}^{-1}3d_{5/2}^{-1}4s)_{J=7/2} \rightarrow (3d_{3/2}^{-1})_{J=3/2}$	*E*2	2632.5 ± 0.5	2632.2		2765.6
g	$(3d_{5/2}^{-2}4s)_{J=1/2} \rightarrow (3d_{5/2}^{-1})_{J=5/2}$	*E*2		2654.0		2788.2

served in our spectra is given in Table I.

Sulfur was introduced into the trap, and the sulfur Lyman-α lines were used as wavelength standards to calibrate the 3-4 spectra. The transition energies of the Lyman lines were set to 2622.10 and 2619.70 eV in accordance with the calculations of Johnson and Soff [10]. The measured energies of the *M*3 and *E*2 transitions in Th^{62+} and U^{64+}, as well as those of adjacent transitions in copperlike and cobaltlike ions observed in the high-resolution spectra, are given in Table I. The error limits typically range between 0.2 and 0.3 eV. For the nickel-like lines the error limits are due to uncertainties in the geometrical distances used to calculate the dispersion, as well as nonlinearities in the position response of the resistive-wire detector. The error limits of the weaker cobaltlike and copperlike lines (especially in the uranium measurement) are also affected by counting statistics. Comparing with our calculated values we find close agreement, which further supports our line identifications. The calculated values are between 0.3 and 1.5 eV smaller than measured. Exceptions are the copperlike *E*, which measured 2.5 eV higher than the value calculated for U^{63+} and 3.0 eV higher for Th^{61+}, and the blend of cobaltlike lines $a+b$, which in U^{64+} measured about 1 eV smaller than calculated. The large discrepancies for line *E* can be attributed to its two-electron–one-photon nature. The calculation of this level depends sensitively on the treatment of configuration interactions, so that the accuracy of the calculations is reduced from that for other levels that mix less.

A comparison of the measured and calculated relative intensities of the nickel-like *M*3 and *E*2 lines from U^{64+} is given in Table II. The calculations predict a decreasing ratio resulting from relative changes of the electron-impact excitation cross sections of the levels feeding the *M*3 and *E*2 transitions. By contrast, the experimental ratio increases with electron-beam energy, even as the ionization threshold of U^{64+} at 7.4 keV is crossed. The difference can be attributed to radiative cascade feeding from levels with $n > 5$, which were not included in the model, and, for beam energies above the ionization potential, to ionization and recombination processes. The processes of charge exchange between ions in the next higher charge state and neutral ambient gas and of inner-shell ionization of the next lower charge state were shown to be major population mechanisms of the lowest excited level in the closed-shell neonlike ion [11]. These processes may also preferentially populate the lowest excited level in nickel-like ions, and their presence would explain the large relative intensities at 8.0 and 9.2 keV. By contrast, dielectronic processes cannot contribute to the excitation of the nickel-like transitions above the ionization potential.

The lowest excited level in a highly charged heliumlike ion (filled *K* shell) decays by an *M*1 transition, that in a neonlike ion (filled *L* shell) by an *M*2 transition, and that

TABLE II. Comparison of measured intensity ratio *M*3/*E*2 in nickel-like U^{64+} with calculations for various electron-beam energies.

E_{beam} (keV)	$I_{expt.}$	$I_{theor.}$
6.2	0.67	0.77
7.2	0.71	0.73
8.0	0.79	0.70
9.2	0.90	0.66

in a nickel-like ion (filled M shell) by an $M3$ transition. It is natural to assume that the lowest excited level in a neodymiumlike ion (filled N shell) decays by a magnetic hexadecapole ($M4$) transition. We have made structure calculations of the most highly charged neodymiumlike ion that we can investigate in EBIT, i.e., U^{32+}, and its lowest excited level, $(4f_{7/2}^{-1}5s)_{J=4}$, indeed connects to the $^1S_0$ ground state via $M4$ decay. Moreover, the second lowest excited level, $(4f_{7/2}^{-1}5s)_{J=3}$, connects to the ground state via electric octupole ($E3$) decay. The calculated transition rates are, however, prohibitively small, namely, 3.3×10^{-7} and 1.8×10^{1} s^{-1} for the $M4$ and the $E3$ transition, respectively, and we do not expect that these transitions will be observed in any currently available device.

In summary, the low-energy region of the 3-4 transitions in near-nickel-like thorium and uranium has been investigated, and the first observation was made of magnetic octupole decay in an atomic system. The transition energies of the $M3$ lines in Th^{62+} and U^{64+} were measured with a precision of 80 ppm. The $M3$ line is not directly excited by collisions. Instead, model calculations show that the transition is almost exclusively fed by radiative cascades from higher levels. Observed relative intensities show reasonable agreement with theoretical results and, for beam energies above the ionization threshold, indicate large contributions from other indirect excitation processes, such as radiative and charge-exchange recombination.

We thank D. Nelson, who assembled the spectrometer, and M. Eckart, R. Fortner, and A. Hazi for their encouragement and support. This work was performed under the auspices of the U.S. Department of Energy by Lawrence Livermore National Laboratory under Contract No. W-7405-ENG-48.

[1] M. Klapisch *et al.*, Phys. Rev. Lett. **41**, 403 (1978); M. Bitter *et al.*, *ibid.* **43**, 129 (1979); E. Källne, J. Källne, and J. E. Rice, *ibid.* **49**, 330 (1982).

[2] A. H. Gabriel and C. Jordan, Nature (London) **221**, 947 (1969); H. R. Griem, Astrophys. J. **156**, L103 (1969); A. H. Gabriel and C. Jordan, Phys. Lett. **32A**, 166 (1970).

[3] J.-C. Gauthier *et al.*, J. Phys. B **19**, L385 (1986); J.-F. Wyart *et al.*, Phys. Rev. A **34**, 701 (1986).

[4] C. L. Cocke *et al.*, Phys. Rev. A **12**, 2413 (1975); D. D. Dietrich *et al.*, *ibid.* **54**, 1008 (1985).

[5] R. W. Dunford *et al.*, Phys. Rev. Lett. **62**, 2809 (1989); P. H. Mokler *et al.*, *ibid.* **65**, 3108 (1990).

[6] I. P. Grant *et al.*, Comput. Phys. Commun. **21**, 207 (1980).

[7] A. Bar-Shalom, M. Klapisch, and J. Oreg, Phys. Rev. A **38**, 1773 (1988).

[8] M. A. Levine *et al.*, Phys. Scr. **T22**, 157 (1988); R. E. Marrs *et al.*, Phys. Rev. Lett. **60**, 1715 (1988).

[9] N. K. Del Grande *et al.*, Nucl. Instrum. Methods Phys. Res., Sect. B **56/57**, 227 (1991).

[10] W. R. Johnson and G. Soff, At. Data Nucl. Data Tables **33**, 405 (1985).

[11] P. Beiersdorfer *et al.*, Phys. Rev. Lett. **65**, 1995 (1990).